*Michael P. Manahan, Sr.**

Plane-Strain Fracture Toughness Determination using Stress Field Modified Miniature Specimens

REFERENCE Manahan, M. P. Sr, **Plane-strain fracture toughness determination using stress field modified miniature specimens,** *Evaluating Material Properties by Dynamic Testing*, ESIS 20 (Edited by E. van Walle) 1996, Mechanical Engineering Publications, London, pp. 177–195

ABSTRACT This paper reports on a new approach† to plane-strain fracture toughness testing. The method enables the testing of specimens which are substantially thinner than those currently believed necessary by the technical community to obtain valid K_{IC} data. The method developed is a direct, experimental approach and does not involve the use of analytical 'correction factors'. The miniature specimen data are compared to data obtained from thermal shock of a 15.24 cm (6 in) pressure vessel. The fracture modes are shown to be identical and the miniature K_{IC} data lie within the experimental scatter of the thick vessel data.

Introduction

Miniaturized specimens are finding a variety of applications in the electrical energy production field. Although size effects in mechanical behaviour testing have been examined for some time, the impetus for miniaturization over the past 15 years was the need to perform post-irradiation testing in a cost effective manner (**1**) to (**2**). Once developed, these tests were used in a variety of non-nuclear applications where sufficient material for conventional testing was either not available or impractical to obtain (**3**) to (**14**). In the case of fracture testing, these applications are also of interest. However, there is an additional purpose for the development of a miniature plane-strain fracture toughness (K_{IC}) test. In high toughness, low strength steels, the thickness requirements for some materials are difficult and very costly to satisfy. In order to address this latter concern, various researchers have attempted analytical corrections to non-conservative data (**7**), (**15**) to (**17**). These attempts have been met with limited success. Many in the technical community are sceptical of these methods and a lively debate has continued for many years on this subject.

As a result of the concerns described above, attention was focused on developing an experimental technique which enables plane-strain fracture toughness testing using specimens with thicknesses less than that currently

* MPM Research & Consulting, PO Box 840, 915 Pike Street, Lemont, Pennsylvania 16851, USA.
† The techniques described in this paper are protected by US patent number 4,895,027 entitled, 'Determining Plane Strain Fracture Toughness and the J-Integral for Solid Materials Using Stress Field Modified Miniature Specimens.'

thought necessary to achieve plane-strain fracture toughness. In particular, a test has been developed which yields valid K_{IC} data using specimens which are substantially thinner than 2.5 $(K_{IC}/\sigma_y)^2$.

One application for this new technology will be in the area of residual plant life assessment. In such applications, only limited quantities of material can be cut from in-service structures. In the nuclear industry, the existing surveillance specimens could be reconstituted and tested to yield fracture toughness data in addition to Charpy data. Three point bend specimens can be weld reconstituted and the modifications described in this paper can then be made to the reconstituted specimen. This approach would enable the measurement of plant-specific K_{IR} curves directly.

Stress field modification theory

With regard to critical fracture toughness testing parameters, ASTM E-399 (**18**) requires

$$B,a_o > 2.5\left(\frac{K_{IC}}{\sigma_y}\right)^2, \tag{1}$$

and ASTM E-813 (**19**) requires

$$B,b_o > 25\frac{J_{IC}}{\sigma_y} \tag{2}$$

where

B = specimen
b_o = uncracked ligament length
a_o = initial crack length
σ_y = effective yield strength

The semi-empirical relationship in (**18**) was determined by an ASTM committee using data such as that given in Fig. 1. The J-integral procedure enables testing with samples that are thinner by about a factor of 20. Logsdon (**20**) has clearly demonstrated that testing using the J-integral procedure yields data identical to that obtained using ASTM (**18**) procedures over the temperature range of validity for that procedure.

This paper reports on a new concept for fracture toughness testing. As shown schematically in Fig. 2, the new test is applicable for specimen thicknesses where plane stress data would be obtained using conventional methods. The basic idea is to modify the stress field in the vicinity of the crack tip to produce plane-strain conditions. The side-pull approach uses force to provide constraint and, in effect, replace the need for material constraint. The side-constraint approach uses material, which is welded on the specimen sides, to produce the needed constraint to achieve plane strain conditions. These

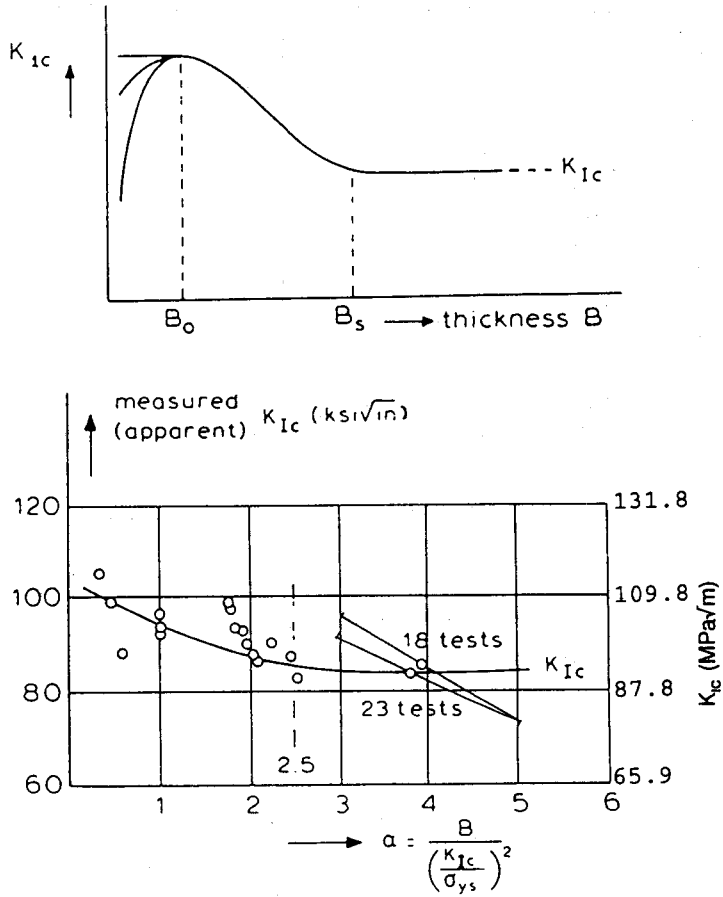

Fig 1 The effect of specimen thickness on the measurement of plane-strain fracture toughness (21)

approaches enable plane strain testing of very thin specimens. At present, the lower limit on thickness has not been determined.

There are several experimental procedures that can be used to modify the stress field. In the current study, side-constraint arms were integrally machined to simulate welded arms attached to pressure vessel surveillance specimens. Future studies will focus on solving problems associated with welding the side-constraint arms in place. The size of the arms and placement on the specimen are critical parameters in successful miniature specimen testing. Figure 3 shows the specimen design.

In order to determine the critical experimental parameters and to validate the basic approach, two- and three-dimensional finite-element model (FEM) analyses were performed. Hence, the benchmark solution is a two-dimensional

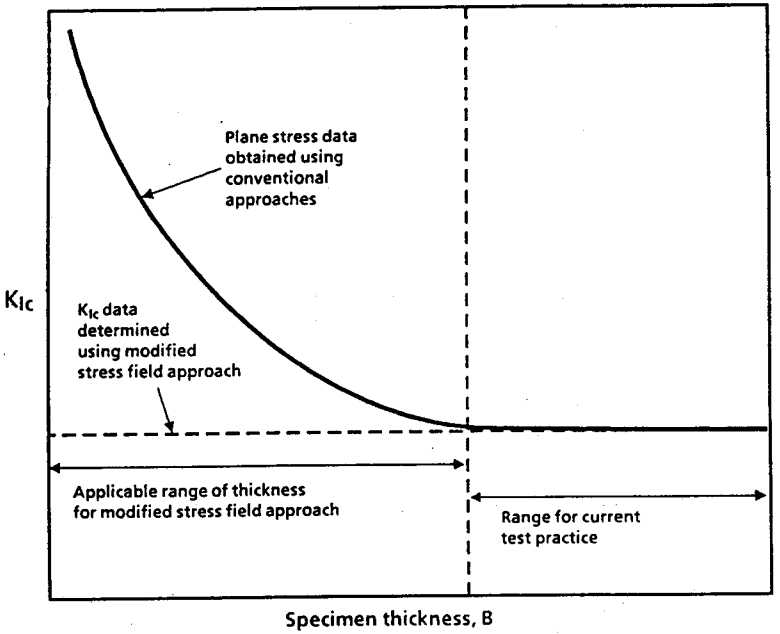

Fig 2 Schematic representation of the range of specimen thickness (B) for which miniature specimens are used

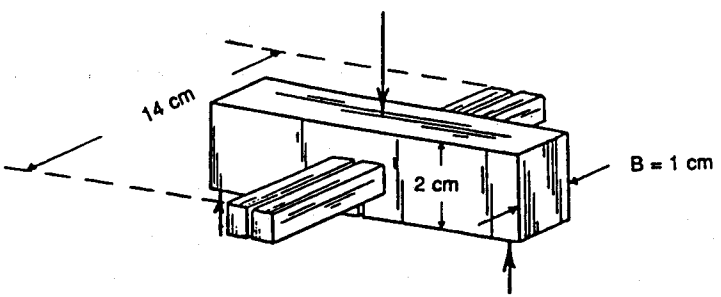

Fig 3 Miniaturized fracture toughness specimen design

plane-strain analysis of the miniature three-point bend specimen. To validate the approach, a three-dimensional finite-element analysis of the three-point bend specimen was performed, in which the side-constraint arm was modelled so that the out-of-plane displacements on the surface are prohibited. Thus, an

approximated local plane-strain condition that retains a triaxial stress state at the crack tip is achieved in the miniature specimen.

Elastic FEM solutions

The reference formulae from the load-point displacement, the crack mouth opening, and the opening mode stress-intensity factor were reported in (**22**) and (**23**) along with a comparison of the finite-element elastic solution. The key results are presented in Table 1.

The displacement solutions for the two-dimensional and the three-dimensional analyses agreed well. These solutions also agreed with the analytical load-point displacement data. The *J*-integral calculated using the two-dimensional contour integral and the virtual crack-extension (VCE) method both agreed with the analytical data to within a few percent. The approximate *J* estimated from the load versus displacement results, however, yielded data 12 percent higher than the analytical value. The accuracy of the approximated *J* is improved as the plastic deformation increases. These results are discussed further below.

Inelastic FEM solutions

The accuracy of the *J*-integral calculation in terms of its path independence for the two-dimensional analysis was evaluated. Good agreement between the *J*-integral data and the virtual crack-extension data was observed. Figure 4 is a plot of the load-versus-load-line displacement for the two-dimensional plane-strain analysis and the three-dimensional analysis. As anticipated, the constrained three-dimensional results are slightly softer than the two-dimensional plane-strain results, but the three-dimensional constrained data are very close to the plane-strain conditions. This result indicates that approximate plane-strain conditions were achieved using the side-constraint technique. On the other hand, the unconstrained three-dimensional results are about 12 percent lower in load, showing this case is rather close to the two-dimensional plane-stress conditions.

The three-dimensional finite-element data are compared with the contour *J* and VCE *J* for the two-dimensional analyses in Figs 5 and 6. The results in these two figures show that the approximate formula for *J* for the constrained three-dimensional model agrees well with the rigorous plane-strain J data. Both of these curves agree well with the side-constraint data.

In addition to verifying the side constraint theory using the integral parameters discussed above, the crack tip region stress contour data were also evaluated. A comparison of the stress contour data for the cases with side constraint and without indicates that the zone of intense plastic flow in the vicinity of the crack tip is smaller for the side-constraint case. This result is expected since material constraint enhances triaxiality and thus prevents

Table 1 Verification of the elastic FEM solutions at an elastic loading of P/B = 14 000 lb/in. (250 kg/cm)

	Reference equations	*Two-dimensional plane strain*	*% Variance from reference equation*	*Three-dimensional with side-constraint*	*% Variance from reference equation*
Load-Point Displacement in. (cm)	1.770×10^{-3} (4.50×10^{-3})	1.800×10^{-3} (4.59×10^{-3})	+2.15	1.808×10^{-3} (4.59×10^{-3})	+2.15
Crack mouth Opening Displacement, in. (cm)	1.065×10^{-3} (2.71×10^{-3})	1.053×10^{-3} (2.67×10^{-3})	−1.13	1.087×10^{-3} (2.76×10^{-3})	+2.07
J, lb/in. (kJ/m^2)	5.88 (1.03) $\left(J = \frac{K_I^2}{E'}\right)$	5.77 (1.01)	−1.87	6.623 (1.16) $\left(J = \frac{2W_1}{B(W-a)}\right)$	+12.6

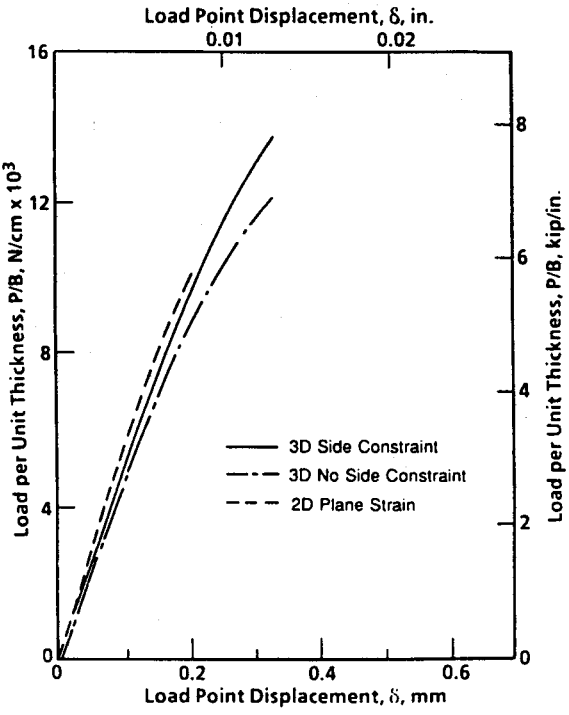

Fig 4 Load per unit thickness versus load-point displacement for two- and three-dimensional finite-element analyses

yielding by increasing the hydrostatic stress. This will reduce the plastic zone size.

Experimental design

As mentioned earlier, there are various experimental procedures that can be used to modify the stress field. In all tests reported here, side-pull arms or side-constraint arms were used to provide constraint and/or to transversely load the specimen and prevent lateral contraction. The definition of plane strain can be considered to be a zero displacement side-surface boundary condition. This condition was achieved experimentally using the side-pull or side-constraint arms. In the current study, the side arms were machined as part of the specimen. Work is currently under way to demonstrate the feasibility of using laser welding to attach the side-constraint arms to a Charpy specimen. This work will be reported in a future publication.

A photograph of the specimens studied is given in Fig. 7. Prior to testing, the specimens were precracked, and the electric-potential (EP) technique was used to monitor crack growth. During fracture testing, EP was used to indicate

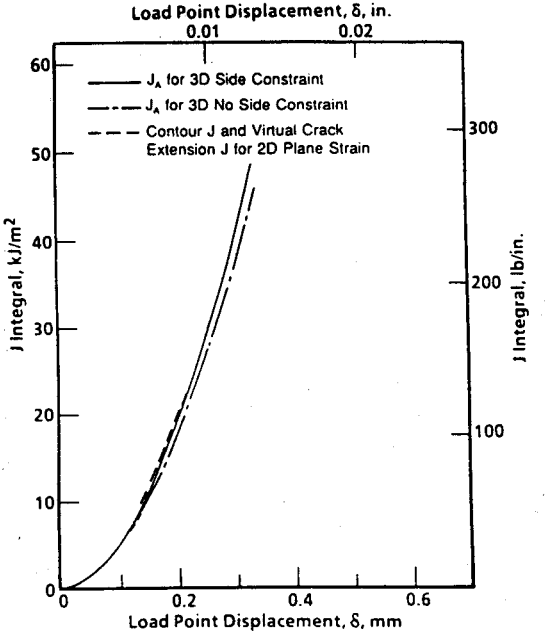

Fig 5 ***J*-integral versus load-point displacement for two- and three-dimensional finite-element analyses**

crack initiation and growth. During the test, load, load-point displacement, EP, crack mouth opening displacement (*CMOD*), and lateral contraction/expansion were measured. In essence, the tests were conducted using instrumentation which satisfied the requirements of both ASTM E399 and ASTM E813.

The specimens were fabricated from a nuclear-grade ASTM A508 steel. This steel came from the TSE 6 vessel which was part of the Oak Ridge National Laboratory (ORNL) pressurized thermal shock study (**24**). Mechanical behaviour data, including large-cylinder data, are provided in (**24**).

In order to perform the side-pull experiment, two load-trains are required: one mounted vertically and the other mounted horizontally. The experimental setup is shown in Fig. 8. Prior to testing, finite element analyses were performed to design the specimen and to determine the required horizontal load as a function of vertical loading to maintain plane strain conditions. These data are shown in Fig. 9.

An important experimental concern is to preserve the specimen's rotational and translational degrees of freedom during the test. Therefore, it is necessary to ensure that the specimen side-load arms do not contact during the test. This would result in a nonphysical constraint and would short out the EP system. A

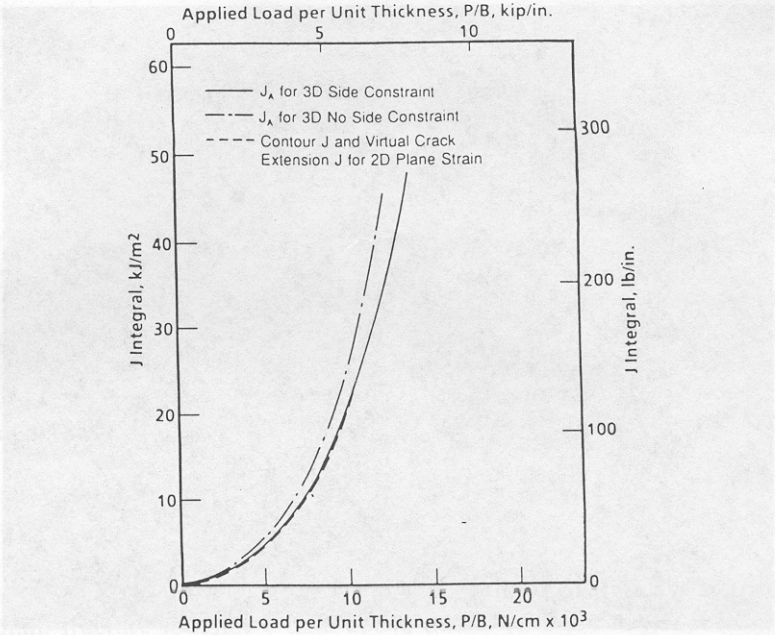

Fig 6 *J*-integral versus applied load per unit thickness for two- and three-dimensional finite-element analyses

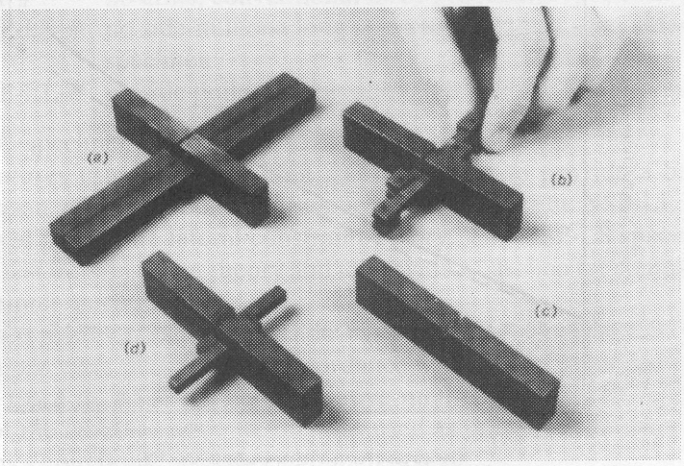

Fig 7 Miniature fracture toughness specimens

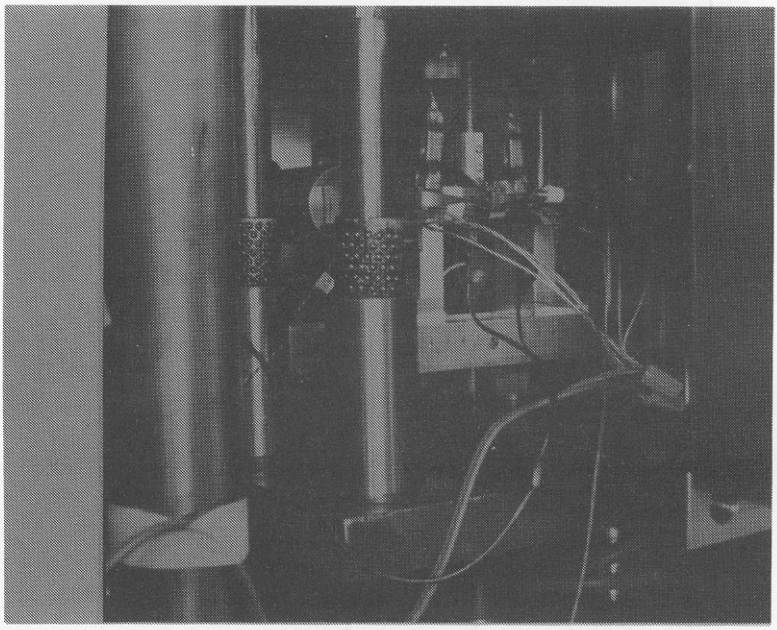

Fig 8 Side-load apparatus for miniature fracture toughness specimen testing

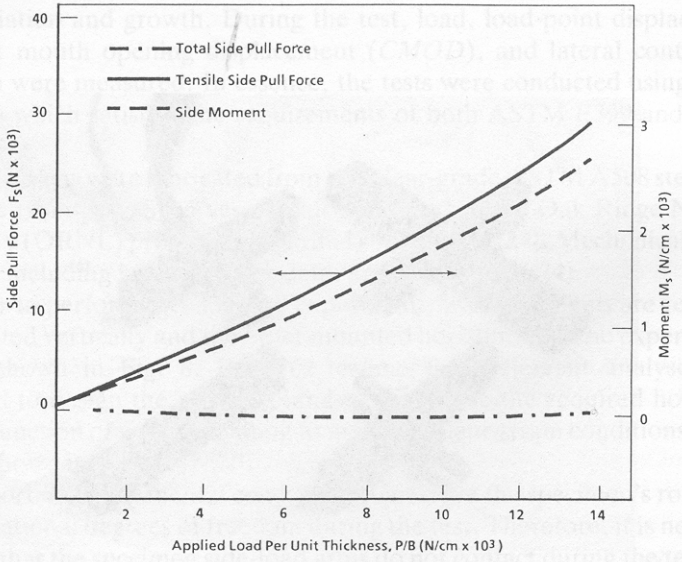

Fig 9 Side-pull force as a function of applied load required to achieve near plane-strain conditions

universal joint was used in the side-load fixturing so that the side-load arms could deflect and rotate.

Data analysis

Material characterization

In order to verify that a portion of the TSE 6 vessel tested was well represented by the data in (**24**), tensile tests were conducted. The results, which are reported in Table 2, compared well with the data in (**24**).

Since the goal of the present work is to demonstrate experimentally that cleavage is obtained in a stress field modified miniature specimen at a temperature where specimens of the same thickness do not cleave, it is important to choose the test temperature with care. As shown in Fig. 10, the ORNL Charpy data show that the transition region ranges from about −20 to 100°C (−4 to 212°F). As discussed in (**4**), the static to dynamic translation is about 40°C (104°F). Therefore, for static fracture toughness testing, and with the goals of the present study in mind, the transition region range of interest is 0 to 60°C (32 to 140°F) to focus on the higher temperature transition region. Examination of the ORNL fracture toughness data (Fig. 11) shows that it was not possible to obtain fracture toughness data above about 40°C (104°F) within the scatter band of the thick section data using laboratory specimens. Therefore, the temperature range chosen for the modified stress field testing ranged from 27 to 80°C (180.6 to 176°F).

Fracture toughness data

Three specimen types were tested and the following designations were used.

(a) NA-# no arms, conventional three point bend specimen
(b) NSP-LS-# no side-pull/one long arm and one short arm, side-constraint specimen
(c) NSP-LL-# no side pull/two long arms, side-constraint specimen

The NA specimens were used to determine the fracture modes at various temperatures using relatively thin specimens and to provide a baseline for comparison with the modified stress field specimens. The NSP-LL specimens were used to test the lateral constraint theory. The NSP-LS specimens were used to test the constraint theory and to provide a baseline for comparison with the side-pull specimens.

The test results are shown in Table 3 and Fig. 12. As indicated in Table 3, all calculations were performed in accordance with ASTM procedures. Whether ASTM E813 or ASTM E399 calculative methodologies were followed, the width of the crack plane (1.02 cm) was used as the specimen thickness in the mechanics equations. All other parameters have their usual definition.

Specimen NA-1 was tested first at 80°C (170°F). Since ductile tearing was

Table 2 Summary of TSE 6 tensile data

Parameter[a]	*CTD-1*	CTD-2	CTD-3	CTD-4	CTD-5
Test temp °C (°F)	−18	−18	80	135	135
	(0)	(0)	(175)	(275)	(275)
Young's Modulus 10^6 MPa (psi)	0.2	0.2	0.2	0.2	0.2
	(31.9)	(31.1)	(32.7)	(28.7)	(31.6)
Yiled Strength MPa × 10^{-3} (ksi)	696.3	695.6	646.0	632.9	693.5
	(101.0)	(100.9)	(93.7)	(91.8)	(100.6)
Ultimate MPa × 10^{-3} (ksi)	846.6	844.5	785.2	772.1	848.7
	(122.8)	(122.5)	(113.9)	(112.0)	(123.1)
Fracture Strength MPa × 10^{-3} (ksi)	629.4	594.3	581.2	575.0	644.6
	(91.3)	(86.2)	(84.3)	(83.4)	(93.5)
True Fracture Strength MPa × 10^{-3} (ksi)[b]	1367.1	1239.5	1318.1	1322.3	1333.3
	(198.3)	(179.8)	(191.2)	(191.8)	(193.4)
True Fracture Strain %[c]	77.5	72.6	81.9	83.2	72.6
True Fracture Stress[d] (ksi)	168.6	152.8	158.7	163.0	164.4
% RA	53.9	52.0	55.9	56.5	51.6
Elongation % (measured)	20.0	22.6	20.3	18.4	19.4
Elongation % (chart)	20.9	22.0	18.0	18.0	18.3
A_o (in.^{2})	0.1971	0.7192	0.7195	0.1978	0.1978
A_F (in.^{2})	0.09079	0.09457	0.08709	0.08605	0.09566

(a) All tests run at 0.127 mm/mm/min (0.005 in./in./min) past-yield, then the speed increased by factor of 5.
(b) Fracture load divided by A_F.
(c) ln (A_o/A_F).
(d) Bridgeman correction = 0.85 except CTD-3 = 0.83.

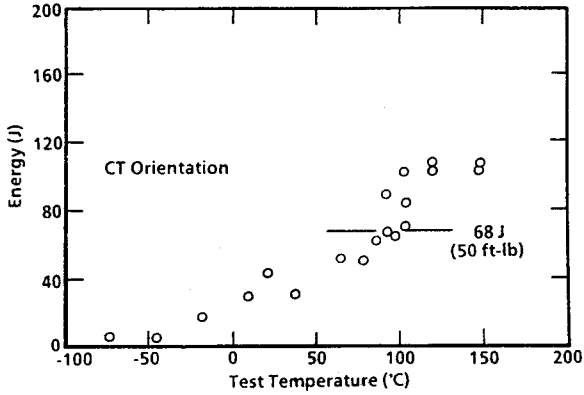

Fig 10 TSE 6 Charpy impact data

observed, we were concerned that this may be the fracture mode in the thick section material at that temperature. Therefore, a decision was made to conduct the next tests at 27°C (80.6°F). Specimens NA-2 and NSP-LS-1 were tested next. Specimen NSP-LS-1 came close to satisfying all of the ASTM E-399 requirements. However, when specimen NA-4 was tested and it was discovered that cleavage occurred in this specimen after a very small amount of stable crack growth, we decided that a more conclusive demonstration of the success of the modified stress field approach would be obtained at 55°C (130.0°F).

Specimen NA-3 was tested next, and this specimen exhibited cleavage after a large amount of ductile tearing. Specimen NSP-LL-1 was tested and cleavage occurred after a very small amount (0.76 mm (0.03 in.)) of stable crack growth. This specimen satisfied all of the ASTM E-399 requirements and yielded a K_{IC} value well within the scatter band of the thick section data. The load versus load-point displacement data for specimens NA-3 and NSP-LL-1 are given in Figs 13 and 14, respectively. Reproducibility experiments were run at 55°C (130.0°F), as shown in Fig. 12, and specimen NA-5 yielded a high K_{JC} value and the fracture mode was entirely ductile. Specimen NSP-LL-2, like NSP-LL-1, exhibited cleavage shortly after peak load. Although this specimen did not satisfy the ASTM E399 P_{max}/P_Q requirement, the fracture toughness data is consistent with the thick section behaviour. Future work should focus on the effects of initial crack length on the fracture toughness results.

The fracture surfaces for specimens NSP-LL-1 and NA-3 are shown in Fig. 15. These specimens were both tested at 55°C. Specimen NSP-LL-1 exhibited cleavage fracture while the fracture for specimen NA-3 was entirely ductile. Thus, the usefulness of the stress field modification approach in producing plane strain conditions in relatively thin specimens has been demonstrated.

Side-pull experiments were also performed at 55°C (131°F) and 80°C (176°F). However, the side-pull grips failed prior to crack initiation. Despite

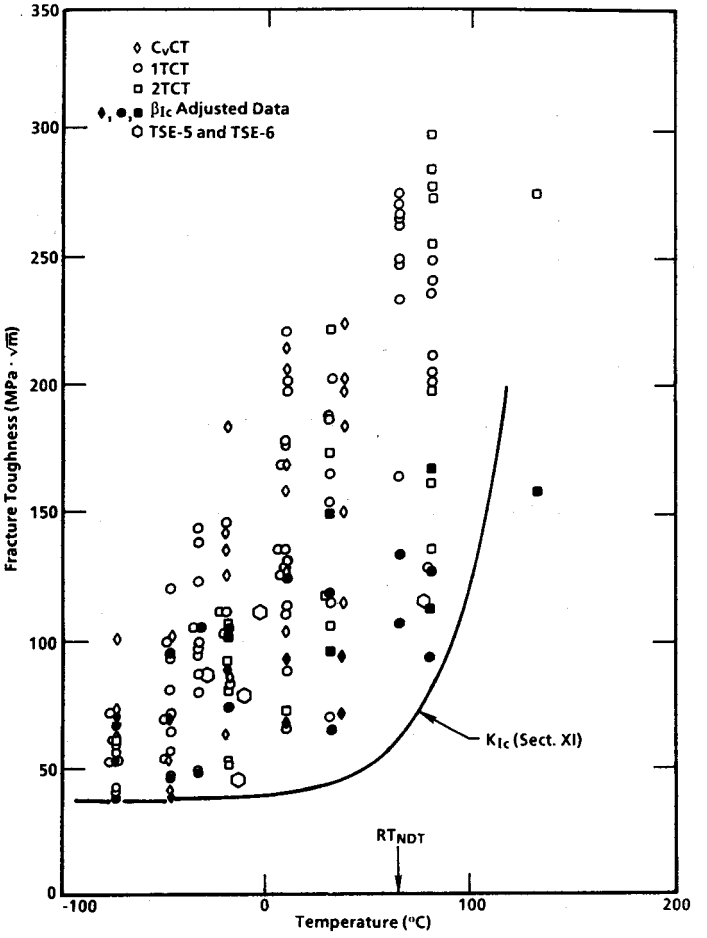

Fig 11 ORNL fracture toughness data for laboratory specimens and thick-section test results for TSE-5 and TSE-6 material

attempts to reconfigure the original design, failure occurred in the last set of experiments around 2268 kg (5000 pounds). A total re-design of the transverse gripping is necessary for future work.

Summary and conclusions

The feasibility of the modified stress field theory has been experimentally demonstrated for an ASTM A508 pressure vessel steel. The basic concept is that the small zone of intense stress in the vicinity of the crack tip controls initiation. Specimen design can achieve a modification of this field to yield

Table 3 Modified stress field fracture toughness data summary

Specimen ID	Test temperature °C (°F)	J_{Ic}[a] kJ/m² (in.-lb/in.²)	K_{Jc}[a] MPa√m (ksi/√in.)	K_{Ic}[a] MPa√m (ksi/√in.)	Thickness requirements B, mm (in.)		ASTM validity requirements satisfied		Fracture mode	Ductile crack length, mm (in.)
					E813	E399	E813	E399		
NA-2	27 (80)	176.1 (1006)	190 (172.9)	–	5.8 (0.23)	n/a	yes	no	ductile, terminated by cleavage	~1.6 (~0.064)
NA-4	27 (80)	126.0 (720)	161 (146.5)	–	4.3 (0.17)	–	yes	no	cleavage after very short ductile crack	~0.5 (~0.02)
NSP-LS-1	27 (80)	162.8 (930)	183 (166.6)	88 (80.1)	5.3 (0.21)	40.6 (1.6)	yes	no[c]	cleavage after short ductile crack	~0.5 (~0.02)
NA-3	55 (130)	266.5 (1523)	235 (213.9)	–	9.1 (0.36)	n/a	yes	no	ductile terminated by cleavage	~6.4 (~0.25)
NA-5	55 (130)	205.3 (1173)	206 (187.5)	–	7.1 (0.28)	n/a	yes	no	ductile	entire ligament
NSP-LL-1	55 (130)	n/a	n/a	91 (82.8)	n/a	45.7 (1.8)	n/a	yes	cleavage after very short ductile crack	~0.8 (~0.03)
NSP-LL-2	55 (130)	n/a	n/a	79[d]	n/a	33.02 (1.3)	n/a	no[d]	cleavage after very short ductile crack	~0.8 (~0.03)
NSP-LS-2	55 (130)	211.6 (1209)	210 (191.1)	–	7.1 (0.28)	n/a	yes	no	ductile	entire ligament
NA-1	80 (175)	249.4 (1425)	226 (205.7)	–	8.9 (0.35)	–	yes		ductile	entire ligament

(a) Determined in accordance with ASTM E813 with initiation detected using electric potential.
(b) Determined in accordance with ASTM E399.
(c) As a result of slippage of the COD gage, the P_{max}/P_Q requirement would not be accurately checked. The equivalent specimen thickness is 0.9 in., which does not satisfy the E399 requirement.
(d) $P_{max}/P_Q = 1.25$.

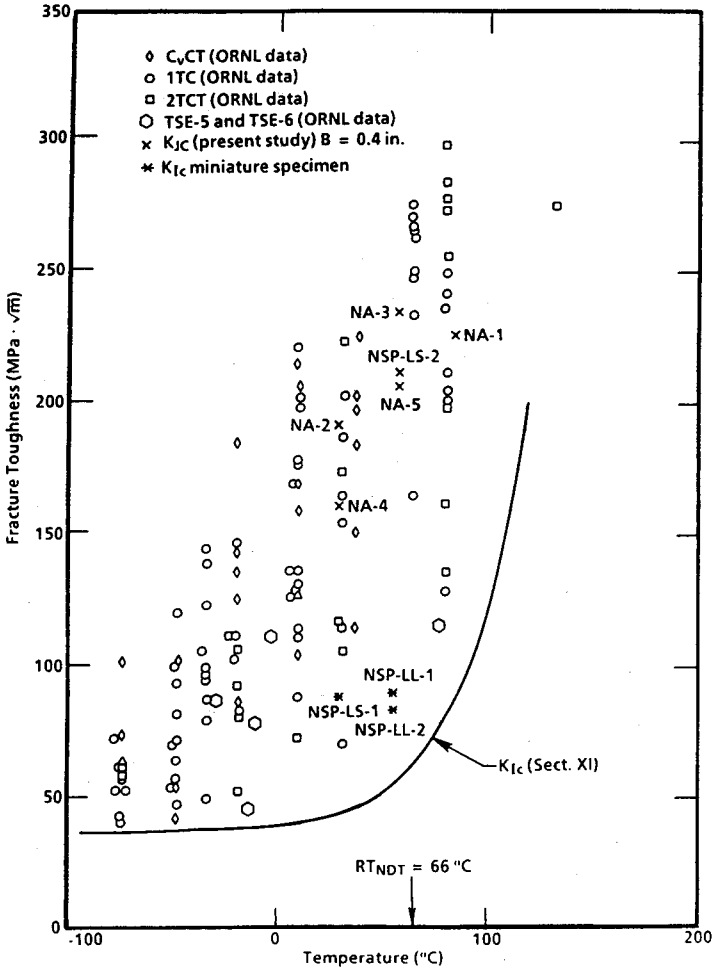

Fig 12 Modified stress field data compared with ORNL thick-section test results for TSE-5 and TSE-6 material

plane-strain behaviour in specimens which would otherwise fracture in plane stress. This approach enables testing specimens which are much thinner than those allowed by current test practices. Future work must focus on demonstrating that valid data can be obtained when side constraint arms are welded in place. If the feasibility of welding the side constraint arms can be shown, then application to irradiated Charpy specimens will enable the direct measurement of K_{IC} as a function of test temperature.

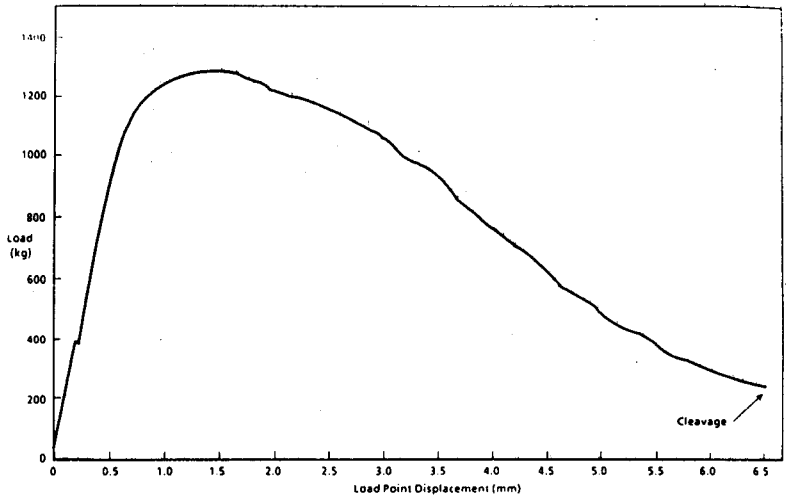

Fig 13 Load vs load-point displacement for specimen NA-3

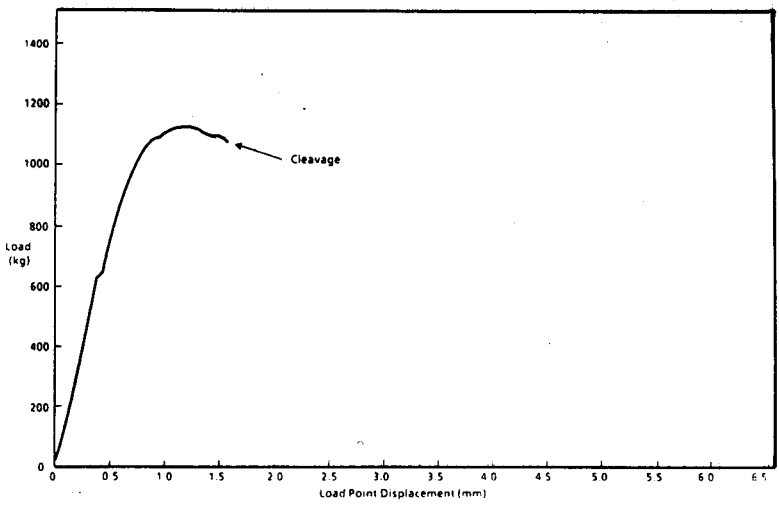

Fig 14 Load vs load-point displacement for specimen NSP-LL-1

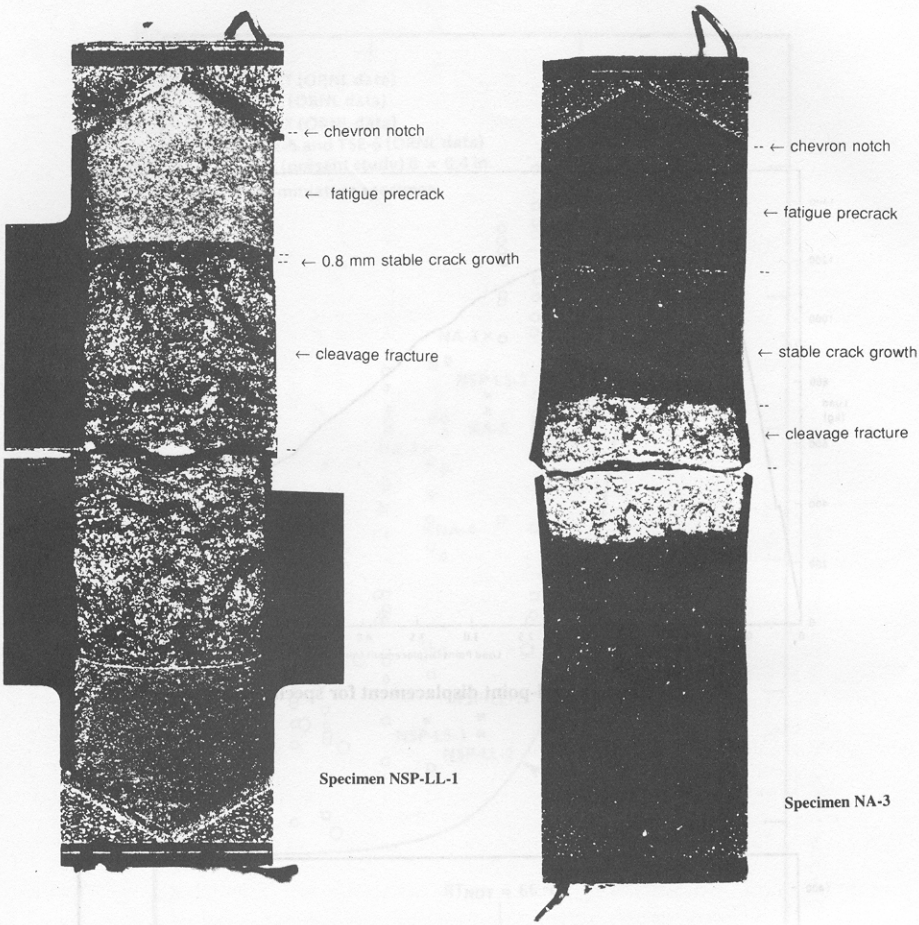

Fig 15 Fracture surfaces for specimens NSP-LL-1 and NA-3 showing cleavage in NSP-LL-1 at a test temperature where ductile fracture would be obtained without the side-arm constraint

References

(1) MANAHAN, M. P., ARGON, A. S., and HARLING, O. K. (1981) The Development of a Miniaturized Disk Bend Test for the Determination of Postirradiation Mechanical Properties, *Journal of Nuclear Materials*, **103** and **104**, 1545–1550, August.

(2) ASTM STP888 (1983) The Use of Small-Scale Specimens for Testing Irradiated Materials, 1983.

(3) MANAHAN, M. P. (1990) Mechanical Behavior of Magnetite From the Oconee-2 and TMI-1 Steam Generators Using Miniaturized Specimen Technology, *Journal of Materials Science*, **25**, 3415–3423, October.

(4) MANAHAN, M. P. and CHARLES, C. (1990) A Generalized Methodology for Obtaining Quantitative Charpy Data From Test Specimens of Nonstandard Dimensions, *Journal of Nuclear Technology*, **90**, 245–259, May.

(5) MANAHAN, M. P. (1990) Thermal Expansion and Conductivity of Magnetite Flakes Taken From the Oconee-2 Steam Generator, *Journal of Materials Science*, **25**, 3424–3428, October.

(6) MAJAMDAR, B., JASKE, C. E., and MANHAN, M. P. (1990) Determining Creep-Crack-Growth Behavior Using Miniature Specimens, *International Journal of Fracture Mechanics*.
(7) MANAHAN, M. P. (1989) Determination of Fracture Behavior of Ferritic Steel Using Miniature Specimens, *Journal of Nuclear Materials*, **166**, 321–330.
(8) MANAHAN, M. P. (1989) Mechanical Behavior and Swelling of Tube Scale From a Pressurized Water Reactor Steam Generator Using Miniature Specimens, *Journal of Nuclear Materials*, **168**, 178–187.
(9) MANAHAN, M. P. (1989) Determining the Physical Properties of Steam Generator Tube Scale Using Miniature Specimens, *Journal of Nuclear Technology*, **85**, 324–333, June.
(10) MANAHAN, M. P., KOHLI, R., SANTUCCI, J., and SIPUSH, P. (1989) A Phenomenological Investigation of In-Reactor Cracking of Type 304 Stainless Steel Control Rod Cladding, Invited Paper, *Journal of Nuclear Engineering and Design*, **113**, 297–321.
(11) MANAHAN, M. P. *et al.* (1988) *Fracture Toughness of Irradiated ASTM A212B Pressure Vessel Steel*, Final Report from Battelle Memorial Institute to OECD Halden Reactor Project, September.
(12) MANAHAN, M. P. (1987) *Surveillance Capsules A' and C' for Nine Mile Point Unit 1*, Final Report from Battelle Memorial Institute to Niagara Mohawk Power Corporation, September.
(13) MANAHAN, M. P. (1983) A New Postirradiation Mechanical Behavior Test – The Miniaturized Disk Bend Test, Invited Paper at the 1982 American Nuclear Society Winter Meeting in Washington, D.C., *Journal of Nuclear Technology*, **63**, 295–315, November.
(14) MANAHAN, M. P., WILLIAMS, J., and MARTUKANITZ, R. P. (1993) Laser Weld Reconstitution of Conventional Charpy and Miniaturized Notch Test (MNT) Specimens, Invited Paper presented at ASTM Symposium on *Small Specimen Test Techniques Applied to Nuclear Reactor Vessel Thermal Annealing and Plant Life Extension, ASTM STP 1204*, (Edited by W. R. Corwin, F. M. Haggag, and W. L. Server) American Society for Testing and Materials, Philadelphia, 199–213.
(15) IRWIN, G. R., KRAFT, J. M., and WELLS, A. A. (1987) *Basic Aspects of Crack Growth and Fracture*, Naval Research Laboratory, NRL Report 6598, November.
(16) MERKLE, J. G. (1984) *An Examination of the Size Effects and Data Scatter Observed in Small-Specimen Cleavage Fracture Toughness Testing*, Oak Ridge National Laboratory, NUREG/CR-3672, ORNL/TM-9088, April.
(17) ROSENFIELD A. R. and SHETTY, D. K. (1984) *Elastic-Plastic Fracture Test Methods: The User's Experience*, ASTM STP 856, (Edited by E. T. Wessel and F. J. Loss) American Society for Testing and Materials, Philadelphia, 196–206.
(18) ASTM Standard E399, Plane-Strain Fracture Toughness of Metallic Materials, American Society for Testing and Materials, Philadelphia.
(19) ASTM Standard E813, Test Method for J_{IC}, a Measure of Fracture Toughness, American Society for Testing and Materials, Philadelphia.
(20) LOGSDON, W. A. (1976) Elastic-Plastic (J_{IC}) Fracture Toughness Values: Their Experimental Determination and Comparison with Conventional Linear Elastic (K_{IC}) Fracture Toughness Values for Five Materials, *Mechanics of Crack Growth*, ASTM STP 590, American Society for Testing and Materials, Philadelphia.
(21) BROEK, D. (1986) *Elementary Engineering Fracture Mechanics* 4th Rev. Ed., Dordrecht: Martinus Nijhoff, **184**, 116.
(22) BUCCI, R. J., PARIS, P. C., LANDES, J. D., and RICE, J. R. (1972) *J* Integral Estimation Procedures, *Fracture Toughness Part II*, ASTM STP 514, American Society for Testing and Materials, Philadelphia, 40–69.
(23) TADA, H., PARIS, P. C., and IRWIN, G. R. (1973) *The Stress Analysis of Cracks Handbook*, Del Research Corp.
(24) CHEVERTON, R. D. *et al.* (1985) *Pressure Vessel Fracture Studies Pertaining to the PWR Thermal Shock Issue: Experiments TSE-5, TSE-5A, and TSE-6* NUREG/CR-4249, May.